LUNAR HYPERSPECTRAL MEASUREMENTS: INSTRUMENT REQUIREMENT SPECIFICATION AND OBSERVATIONAL STRATEGY FOR LIME

ABSTRACT

This document provides the requirements for hyperspectral measurements of the integrated lunar disk that will allow for improved spectral interpolation of the LIME output.

Carlos Toledano
Morven Sinclair
Chris MacLellan
Pieter de Vis
Agnieszka Bialek
África Barreto
Ramiro González

NPL, VITO, AEMET, UVa

22 June 2022

This document was produced as part of the ESA-funded project “Improving the Lunar Irradiance Model of ESA” under ESA contract number:

Signatures and version history

	Name	Organisation	Date
Written by	Carlos Toledano	UVa	18 November 2021
Reviewed by (consortium)		NPL, VITO, AEMET	23 November 2021
Laboratory results added	Morven Sinclair, Chris MacLellan	NPL	05 April 2022
Revied by consortium		NPL, VITO, UVa, AEMET	22 June 2022
Approved by (ESA)	Marc Bouvet	ESA	12 July 2022

Version history

Version	Date	Publicly available or private to consortium?
0.1	23/11/2021	Private
0.2	26/01/2022	Private
0.3	05/04/2022	Private
1.0	12 July 2022	Public

Contents

1 Introduction

1.2 Purpose and Scope

This document provides the requirements for hyperspectral measurements of the integrated lunar disk according to Task 1 .1 of the SoW (AD0). The objective of this measurements is to improve the spectral interpolation of the LIME output at the Cimel lunar photometer spectral bands. The specification of the measurements includes instrument performance requirements, instrument characterisation requirements and the observational strategy.

1.3 Applicable and reference documents

1.3.1 Applicable Documents

The following applicable documents are those specification, standards, criteria, etc. used to define the requirements in this document.

Number	Reference
[AD0]	ESA-EOPG-EOPGMQ-SOW-24. Improving the Lunar Irradiance Model of ESA.

1.4 Glossary

1.4.1 Abbreviations

Abbreviation	Stands For	Notes
ASD	Analytical Spectral Devices	Instrument manufacturer
Cimel	(Not an abbreviation)	Instrument manufacturer, also used as shorthand for instrument itself
DN	Digital Number	
DRF	Directional Response Function	
EO	Earth Observation	
ESA	European Space Agency	Project customer
FOV	Field of View	
FWHM	Full width at half maximum	
GIRO	GSICS Implementation of the ROLO Model	
GSICS	Global Space Based Inter-calibration System	
GUI	Graphical User Interface	
KO	Kick-off meeting	
LIME	Lunar Irradiance Model of ESA	
NPL	National Physical Laboratory	Project partner
QTH	Quartz Tungsten Halogen	
ROLO	RObotic Lunar Observatory	
SNR	Signal to noise ratio	
SoW	Statement of Work	
SRF	Spectral Response Function	
SWIR	Short Wavelength Infrared	
TBX	Toolbox	
TE	Thermoelectric	
TOA	Top of Atmosphere	
UV	Ultraviolet	
UVa	University of Valladolid	Project partner
VITO	Vlaamse Instelling voor Technologisch Onderzoek; Flemish Institute for Technological Research	Project partner
VNIR	Visible and Near Infrared	

2 Instrument performance requirements

As indicated in the SoW, the objectives of this project are to demonstrate an estimated radiometric uncertainty below 2% (*k*=2) for lunar disk irradiance simulations at any wavelength in the spectral range 400 nm to 2500 nm, by making use of hyperspectral measurements of the Moon that allow to spectrally interpolate the current LIME model output at the Cimel lunar photometer spectral bands.

The hyperspectral measurements of the Moon irradiance would ideally provide sufficient spectral information in the range 400 nm-2500 nm to allow interpolation of the LIME model to any desired wavelength or instrument response function, keeping uncertainty of the model output below 2%. Only an instrument which relative spectral radiometric accuracy is well characterised is needed (not its absolute radiometric accuracy), because the hyperspectral measurements are to be used in combination with the irradiance observations provided by a Cimel filter radiometer with an absolute radiometric calibration at 8 spectral narrow bands in the range 440 nm to 1640 nm.

The Cimel radiometer (#1088) was characterized and its irradiance response calibrated by NPL in the previous project (Nº 4000121576/17/NL/AF/hh). A new absolute calibration of this instrument will be carried out in 2022 in the frame of project N. 5001029628, once 2 new channels in the VIS-NIR range are installed in substitution of the UV channels. These absolute calibrations in irradiance were shown to provide the expected low uncertainty at the Cimel bands. The derivation of the uncertainty estimates for the interpolated spectral regions using hyperspectral data will be carried out within this project. Both the measurements and the interpolation strategy will influence the final uncertainty. In this section we will focus on the measurement requirements, whilst tasks 1.3 and 1.4 will tackle the interpolation and uncertainty estimates.

The requirements for the instrument that can be used for the hyperspectral measurements must take into account the uncertainty target and the limitations of the technique to be used, i.e. the application of the Langley plot method to derive the top of the atmosphere lunar irradiance at varying lunar phases. This implies that it will not be possible to obtain data in certain spectral regions affected by strong gaseous absorption by water vapor, oxygen, carbon dioxide, etc. Moreover, a solar irradiance spectrum with certain spectral resolution and uncertainty will need to be used to derive reflectance spectrum.

In order to define the instrument requirements, synthetic data are used. The starting point are the uncertainties of the current LIME model at the 6 Cimel spectral bands[1]. A simulated hyperspectral measurement with a given uncertainty is selected and used to interpolate the model output, using the NPL interpolation tools that are available to the project. The simulated data are presented in Figure 1, where red points represent highly accurate multispectral measurements and the green curve hyperspectral data that has larger relative uncertainties at the level of 5%, (*k*=1). The dashed cyan line shows the results of interpolation that shifts measured low accuracy hyperspectral spectrum to highly accurate multispectral points. We present three cases with different values of hyperspectral data input uncertainties (see

[1] The LIME uncertainty at the Cimel bands can be considered fix although according to Monte-Carlo simulations in LIME-1 project, there is small dependence of this uncertainty on phase angle.

Table 1 for details), but for all cases the combined uncertainty is at the level of 5% threshold.

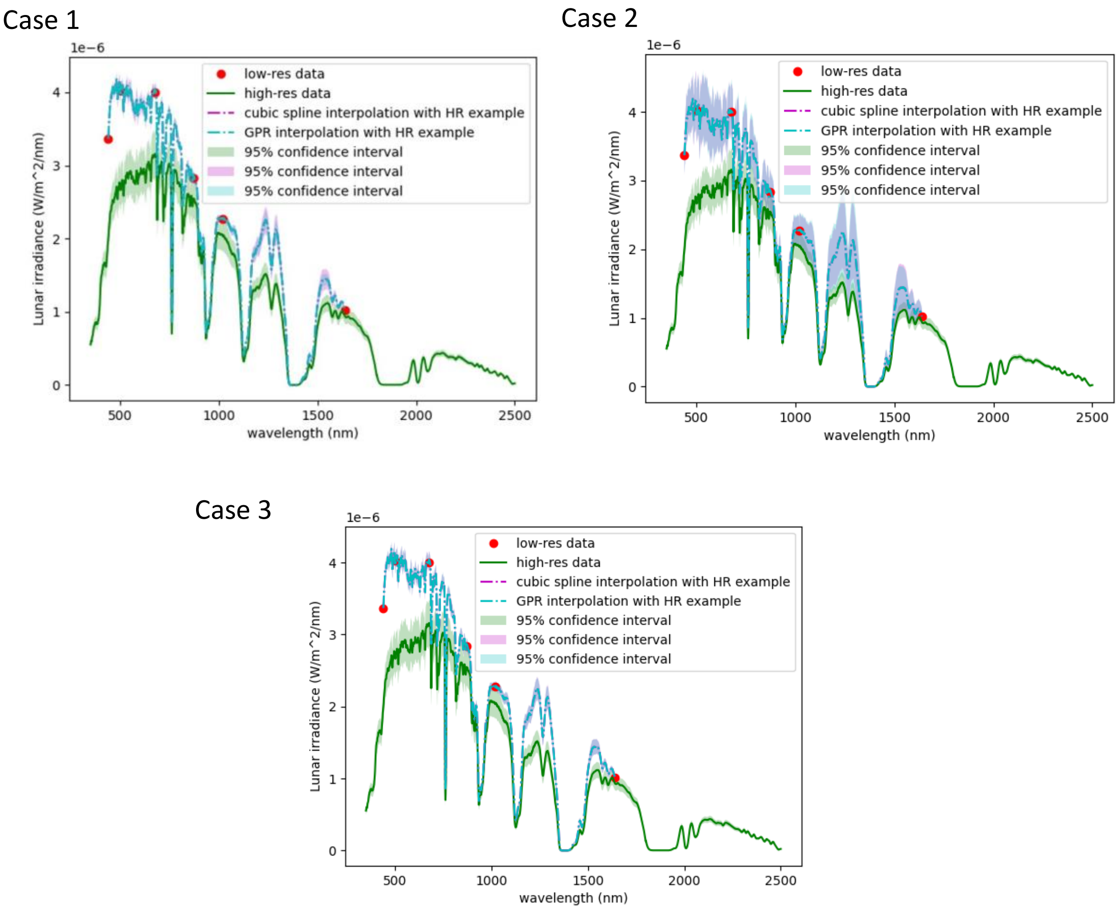

Figure 1. Lunar irradiance. Red points measured full Moon high accuracy multispectral data, green data series simulated hyperspectral measurements with 5% relative uncertainty, dashed violet line cubic spline interpolation of hyperspectral data to fit multispectral points, dashed cyan line is Gaussian process Regression interpolation. Shaded areas of each curve represent 95% confidence interval. Each subplot, case 1, 2 and 3 represents different values of input uncertainty see

Table 1 for details.

Figure 2 presents the uncertainty for the synthetic hyperspectral signal around 5% and the uncertainty of interpolated data using two different methods for case 1, where the uncertainties are reduced to the level of 1% for below 1000 nm. For the wavelength above 1000 nm uncertainties are higher reaching 3.5 %, this is caused by lack of high accuracy multispectral data in that spectral region and anyway any atmospheric absorption wavelengths are likely to be removed from the dataset or will have associated very high uncertainties. However, for case 2 the interpolation process did not reduce uncertainty thus the interpolated spectra still have uncertainty at the same 5% level as the input hyperspectral data. Although the combined uncertainty for case 2 is even slightly lower that for case 1 (5.20% and 5.05% respectively) the contribution of random and systematic uncertainties is different, with the higher contributions of random terms (expressed as noise and partially by radiometric calibration) in case 2. Case 3 has slightly larger uncertainty for interpolated spectrum and here all the input uncertainties are kept as they were in case1 scenario apart from noise that was increased from 0.02% to 0.5%. For case 3 the combined uncertainty is the same as for case 1 but that increase in random contributor visibly increases uncertainty of the interpolated spectrum from 1% level to 1.5%.

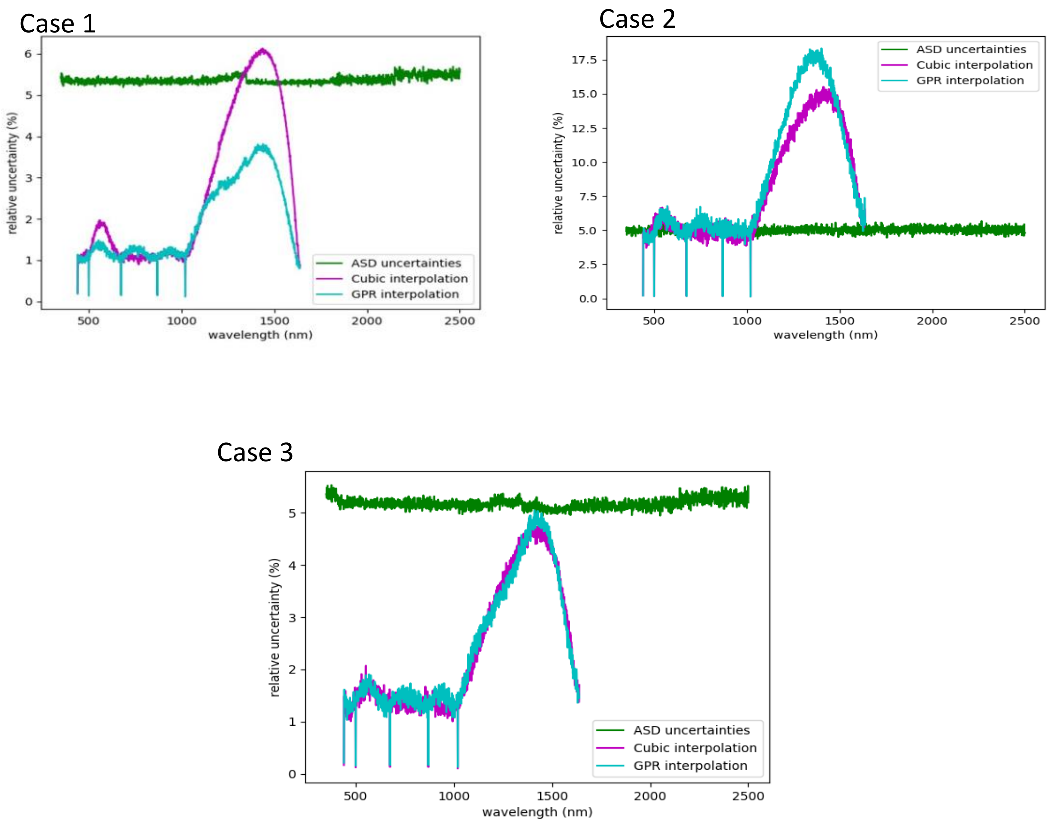

Figure 2. Relative uncertainty of: synthetic hyperspectral measurements (green data series), interpolated data with high accuracy multispectral measurements using cubic method (violet data series) Gaussian process regression (cyan data series). Each subplot, case 1, 2 and 3 represents different values of input data uncertainty see

Table 1 for details

All this in hand, the requirements for the hyperspectral measurements are be based on approximated uncertainty estimates which are at the level of 5%, that allows us to define the instrument requirements at this initial stage of the project.

Table 1 lists a set of basic requirements for the hyperspectral instrument to be used for lunar measurements in the first set of rows, followed by the instrument characteristics with uncertainty values that were used for the interpolation simulations in cases 1-3. Therefore, the final requirement for the hyperspectral instrument should be based on the uncertainty value and type (systematic and random) and this can vary for the same instrument with changing conditions in situ. For example, the noise will vary with the moon phase angle and at some point, might become too high even with long averaging to retrieve usable signal. As a random contributor to overall uncertainty this component will become too high, and the interpolation tool will not be able to retrieve the signal with high accuracy.

Thus, to get small uncertainties on the interpolated hyperspectral data, we need small uncertainties on the CIMEL data (both random and systematic), and small random (with respect to wavelength) uncertainties on the hyperspectral data.

The final uncertainty budget for the LIME output through the entire spectral range will be a result of the WP1 that needs real measurements and calibration.

Table 1.Instrument requirements for hyperspectral measurements for LIME

Characteristic	Value	Comment	
Spectral range	400 nm -2500 nm	SoW	
Field of view	1°	Moon max subtends <0.6	
Spectral resolution	Around 10 nm	Matches current Cimel bandwidth	
	Exemplary uncertainty for 500 nm		
	Case 1	Case 2	Case 3
Relative radiometric uncertainty	0.95%	3.00%	0.95%
Noise	0.02%	3.00%	0.50%
Non-linearity	1.00%	1.00%	1.00%
Stray light	5.00%	2.50%	5.00%
Temperature sensitivity	0.10%	0.50%	0.10%
Total uncertainty	**5.20%**	**5.05%**	**5.20%**

According to the observation strategy (section 4), the spectral response at each phase angle (or interval) will be based on 3 measurements at the most, corresponding to 3 lunar cycles, if the atmospheric conditions are optimum. This is because only one hyperspectral measurement of the lunar irradiance can be derived for each night, using the Langley plot method in a high elevation site like Izaña or Teide Peak observatories.

ASD FieldSpec Pro 4 is a spectroradiometer available on the market that meets the set of general requirements and was chosen to be further used in this study. The set of laboratory tests were performed to verify some of the instrument's characteristics prior to its field installation. Their results are presented in section 3, Instrument Characterization Laboratory Data and together with field data will be used to derive the final uncertainty budget. Section 4, Observational strategy, describes the approach to the field deployment, and Appendix A contains additional information related to instrument FOV tests and ASD preparation for the field deployment, such as environmental enclosure and custom written acquisition software details.

3 Instrument Characterization Laboratory Data

The ASD Fieldspec Pro (FS4) spectroradiometer (Unit #18454) was characterized at the National Physical Laboratory over November/December 2021 the key points will be highlighted and reported here.

3.1 The Instrument

This instrument is designed to be portable and the flexible fiber-optic cable allows for a range of motion during use. Most commonly this is used with a tripod fitting or pistol-grip, allowing the user to freely point at various targets.

Figure 3: ASD FieldSpec Pro 4 and Example of Field Use

The ASD contains 3 spectrometers operating at:

- VNIR 300 nm – 1000 nm
- SWIR 1 1001 nm – 1800 nm
- SWIR 2 1801 nm – 2500 nm

The ASD then uses a third-order polynomial to calibrate the spectral sampling points within each of the spectrometers and interpolates these to a 1 nm interval. It is important to validate this calibration; something which will be examined further in Section 3.5.1.

The specification of the ASD system indicates that this system should be capable of collecting spectral data reflected from the surface of the moon, however the system is designed for near surface downward-facing data acquisition, and it is an unusual application to instead point the system upwards at small targets.

As a result, a significant change to the system is the exchange of the standard 8 ° field of view (FOV) fore-optic for a smaller 1 ° FOV fore-optic to optimise the view of the lunar disc (as discussed in the Project Proposal ESA RFP/3-17088/21/I-DT-Ir CRM31544). Figure 4 displays the size of the lunar disc within the 8 ° FOV and 1 ° FOV, with the positioning of the different spectrometer sensor input fibres relative to this.

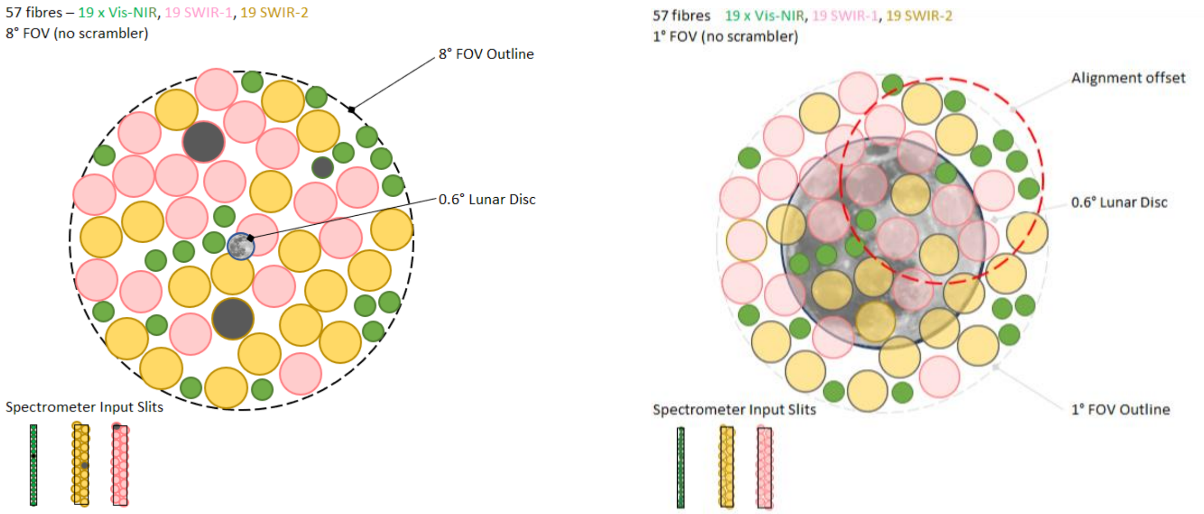

Figure 4: Size of the lunar disk within the field of view using 8° FOV (left) and 1° FOV (right), also showing the position of the individual fibres that return the light to the slits of the three ASD spectrometer inputs (schematic).

Another important change to the standard sampling system is the addition of an optical scrambler light guide. This ensures that all fibres will see the full field of view of the Moon and makes the instrument less sensitive to spatial variation, as well as providing spatial uniformity in the spectral channels. Figure 5 shows the reverse illumination of the VNIR sensor fibres without (left) and with (right) the addition of the scrambler.

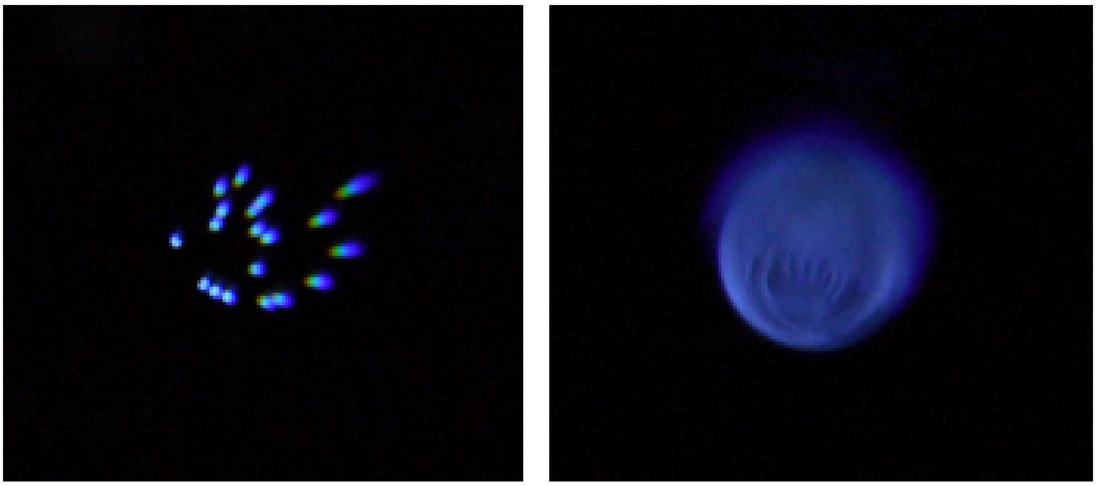

Figure 5: Left: VNIR individual fibers (backlit), Right: VNIR backlit with scrambler fitted

Although these changes in fore-optic improve the system uniformity, the lunar disc is typically 0.6 ° or less within this FOV so additional measurements need to be conducted in order to determine the limitations of underfilling the FOV and its directional response function. This characterisation will be further examined in the sections below.

3.2 Signal to Noise Ratio Measurements

The laboratory signal to noise measurements were based on a lunar simulation using a Quartz Tungsten Halogen (QTH) radiance source at 2000 cdm^{-2}. This was equivalent to an illuminance level of <1 lux at the ASD fore-optic input. An iris aperture was fitted in front of the radiance source to simulate different phases of the moon. The peak raw DN value from the ASD was in the region of 10000 – 35000

DN for the full 1 º FOV and between 1000-5000 DN for <0.5 º FOV (Figure 6). The standard deviation and therefore signal to noise levels are dependent on the ASD sample averaging as well as the difference between the QTH source and the lunar reflected solar spectrum. In addition to this the tracking accuracy and alignment are critical to SNR values and therefore we require field data for realistic values.

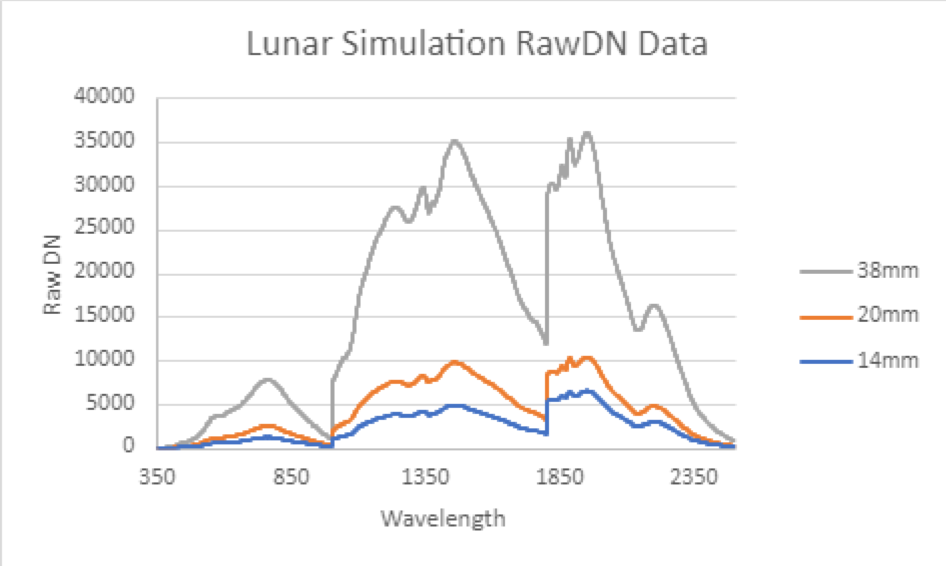

Figure 6: Preliminary lunar simulation over 3 different iris aperture sizes

During laboratory characterization the ASD was set-up to acquire outdoor data one evening (in the UK), using manual alignment of the fore-optic. On March 7th the illumination was 23 % (this is a percentage on the Moon illuminated by the Sun, 100% would be at full moon) and there was thin and partial cloud cover with some cloud breaks. As can be seen in

Figure 7 the attempt to collect field data was difficult and we were unable to yield any realistic SNR values without the lunar tracker and better atmospheric conditions.

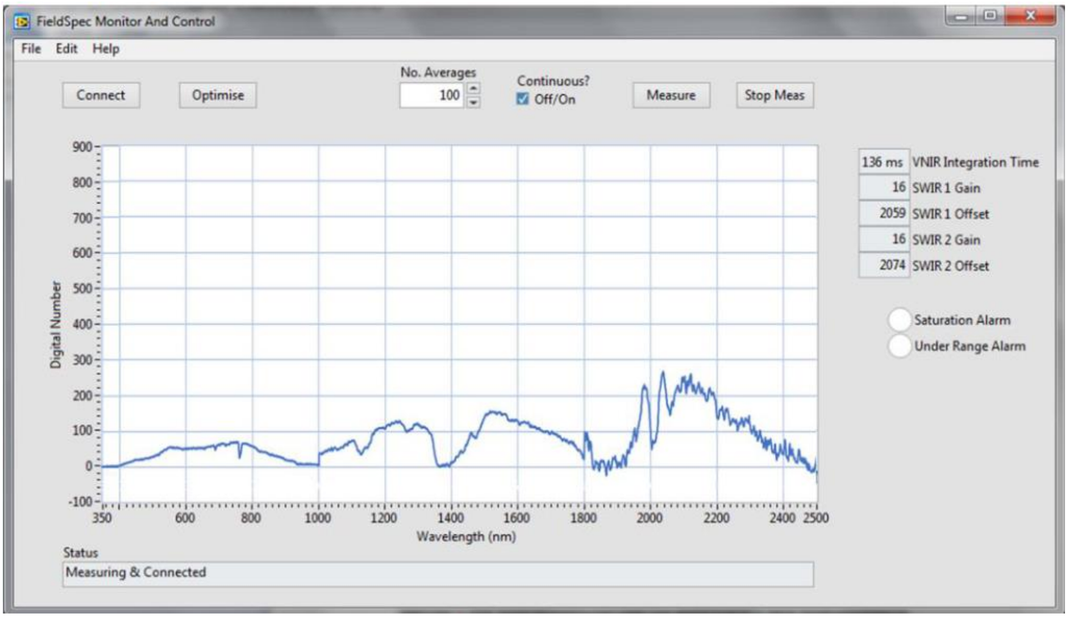

Figure 7: Field data and manual alignment

3.3 Relative Spectral Radiometric Calibration

As described in Section 3.2 the spectroradiometer is only required to have a relative spectro-radiometric calibration. The Cimel measurements are then used to scale the ASD data to absolute spectral irradiance values. A relative radiometric calibration can be achieved by (i) directly viewing an FEL irradiance standard, (ii) viewing a calibrated reflectance panel which is illuminated with the FEL irradiance lamp or (iii) viewing the output from a calibrated radiance sphere source. We have chosen the radiance sphere option for improved measurement repeatability and uncertainty compared to viewing the FEL lamp directly with the ASD 1° fore-optic and its possible non-uniformity directional response function (DRF) issue (see Section 3.6).

The Sphere Optics radiance source used is owned by the National Environmental Research Council and was calibrated against the NPL 2010 spectral irradiance scale and the NPL-traceable 2003 reflectance scale respectively. The sphere port is rectangular and measures 140 mm by 65 mm.

ASD RS^3 Internal Radiometric Calibration Option:

The RS^3 application has a built-in option for calculating calibrated radiance or irradiance values from the raw digital numbers (Raw_DN). System response calibration files are used for each fore-optic accessory. A new calibration file was created for the combination of the 1 ° FOV with scrambler (Figure 8). This also required replacing the factory “ILL” and “REF” files for the NPL calibration radiance sphere source (Figure 9, Figure 10).

Please note that each time the fore-optic and fibre are disassembled the radiometric calibration will change, therefore the preliminary data discussed here is not the final calibration performed prior to imminent field deployment, but instead shows the early testing and method validation.

Calibration file directory: Program Data\ASD\RS3\

Filenames:

LMP184542.ill	Radiance Sphere Source	NPL Radiance Values * π
BSE184542.ref	Reflectance Panel	All values set to 1 (Reflectance panel not used)
11i184542.raw	System Response Calibration file for 1° FOV + Scrambler	

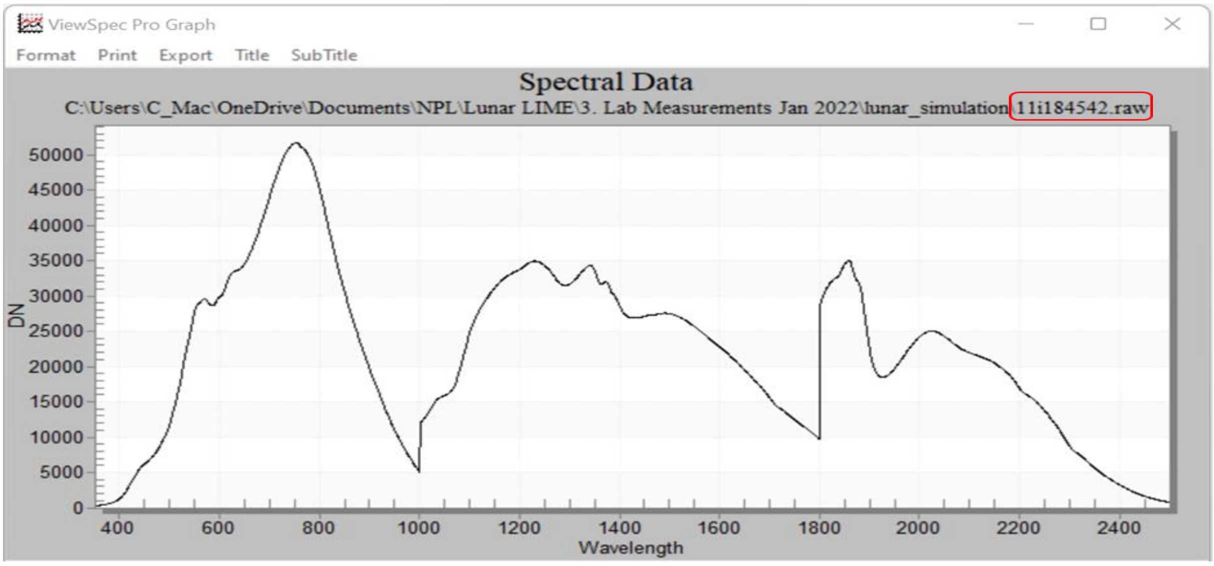

Figure 8: .raw file, System Response Calibration File

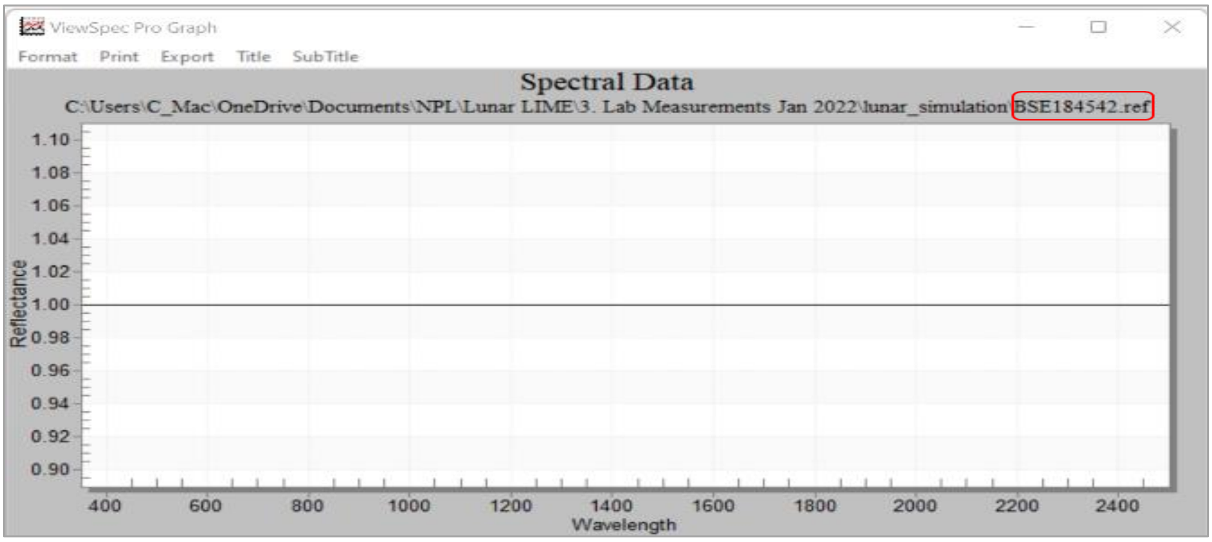

Figure 9: .ref file, Reflectance Panel (Set to 1)

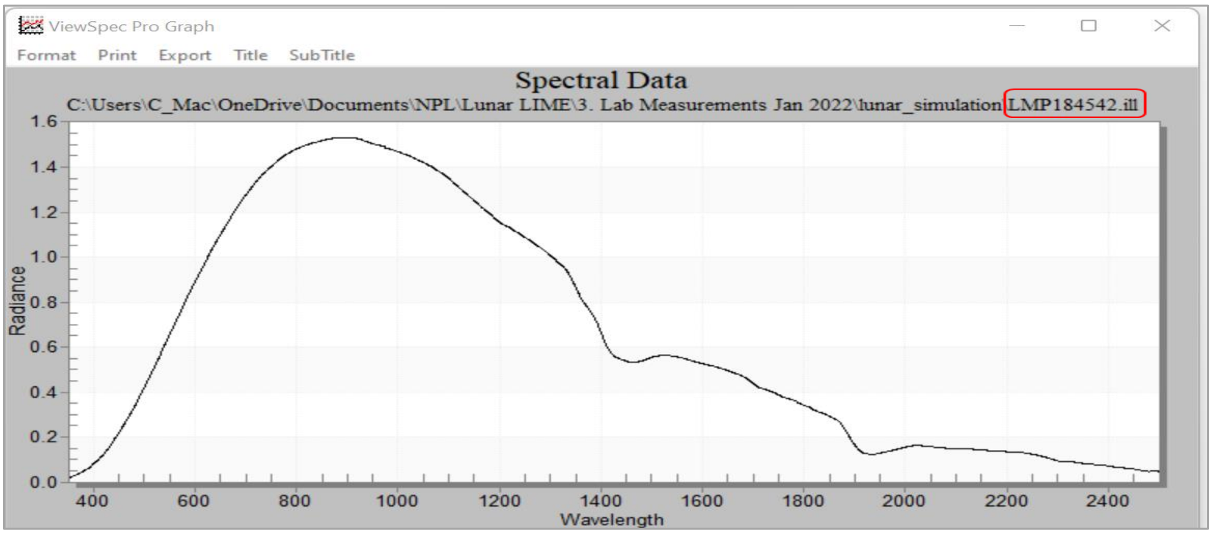

Figure 10: .ill file, Radiance Sphere Source

Activating radiance measurements within RS^3 produces a smooth continuous spectral plot when the FOV is overfilled by the uniform radiance source.

Radiometric Calibration from Raw_DN Data:

It is also possible to calculate spectral radiance from the ASD's Raw_DN values external to the RS^3 application, with the average and standard deviation of this displayed below (Figure 11). All the Raw_DN values acquired by the RS^3 application are dark subtracted. Note that the variation in atmospheric water vapour absorption adds to the calibration uncertainty in these regions.

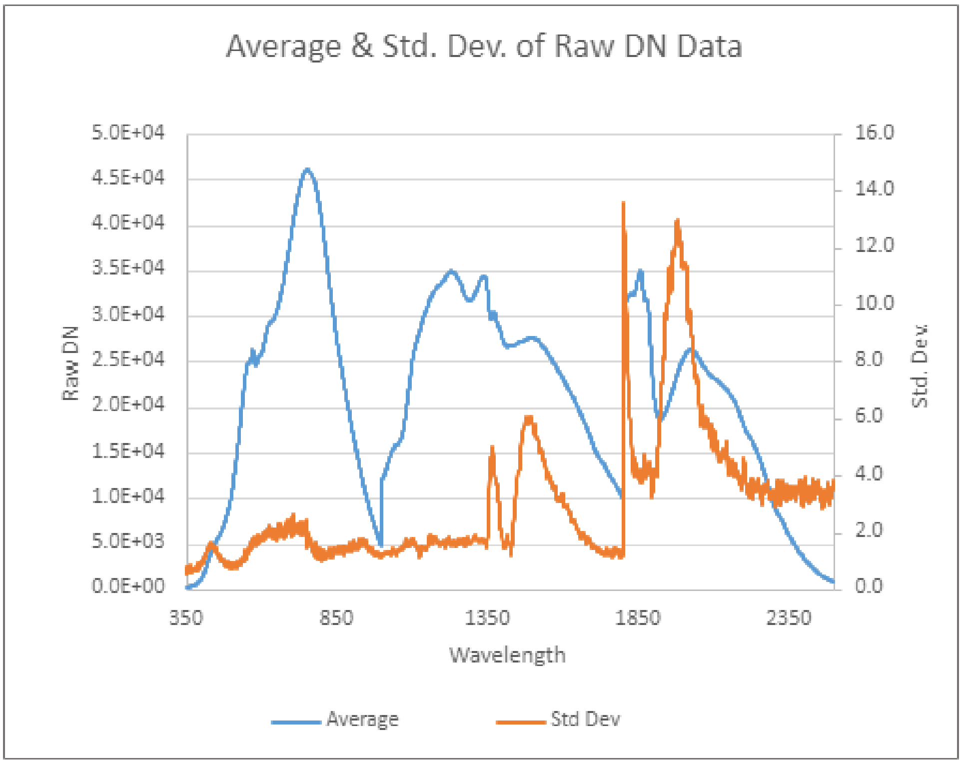

Figure 11: Average and Standard Deviation for RawDN Data from the Radiometric Calibration SRF Example Below

How To Create a System Response Calibration File:

Collect 30 Raw_DN data files of the calibrated radiance sphere source. Convert files to ASCII and import into the Excel spreadsheet:

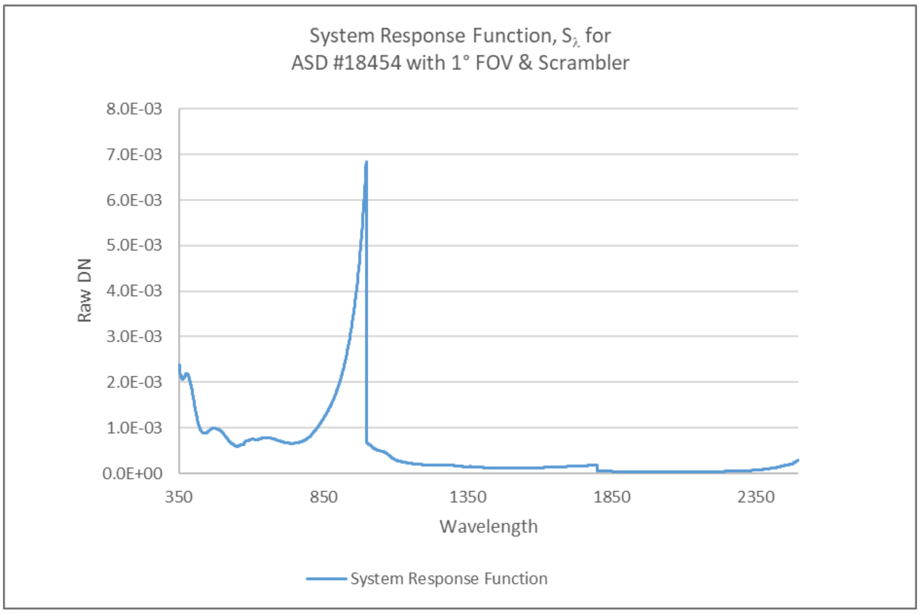

Figure 12: System Response Function 'S' for ASD #18454

The System Response Function (Figure 12) can then be applied to subsequent Raw_DN data files to scale into spectral radiance. Note it is essential to ensure the correct VNIR integration times and SWIR gain factors are included in the calculations. For clarity Equation 1 details the irradiance calculation where radiance is multiplied by π. Within the ASD RS3 software the divisor of π is left out in any calculation of an irradiance measurement as the application can distinguish between irradiance & radiance via the fore-optic specified in the header of the data file[2].

$$L_{\lambda} = \frac{S_{\lambda} * \ RawDN_{(\lambda)}}{Int.Time} \quad (1)$$

$$Radiance_{(\lambda)} = \frac{S_{\lambda} * \ RawDN_{(\lambda)}}{Int.Time \ or \ Gain \ Factor} \quad (2)$$

$$System \ Response \ Function_{(\lambda)} = \frac{Calibration \ Standard \ Value_{(\lambda)} * \ Int.Time \ or \ Gain \ Factor}{RawDN_{(\lambda)}} \quad (3)$$

As mentioned previously the ASD must be housed within its enclosure with the fore-optics permanently fitted before the final radiometric calibration prior to deployment, anticipated to happen late Feb/early March. The radiometric calibration will include an iris aperture to simulate different lunar sizes within the field of view (preliminary discussion of this data in Appendix A). These multiple relative radiometric calibrations can be used to provide the best fit to avoid step discontinuities in the spectral data.

3.4 Solar Spectral Irradiance Measurement

The ASD field spectroradiometer was calibrated with the 1 ° fore-optic and scrambler using the Internal Calibration Option described above. The system, together with a calibrated diffuse reflectance panel, were taken outdoors on a bright sunny morning at NPL (10:55, UTC on 21st January, solar elevation angle =16.8 °). The fore-optic was aligned to view the reflectance panel at nadir and a series of ASD radiance measurements were acquired. The data was converted into ASCII and imported into an Excel spreadsheet:

Using the calibrated reflectance (radiance factors) for the panel it was scaled for spectral irradiance. The spectral irradiance values from the American Society for the Testing of Materials (ASTM) have been linearly scaled to match the ASD irradiance values. This gives a first look at the performance of the ASD and what we might expect from a lunar irradiance measurement.

[2] D. C. Hatchell, "Fieldspec Radiometric Calibrations." ASD Report

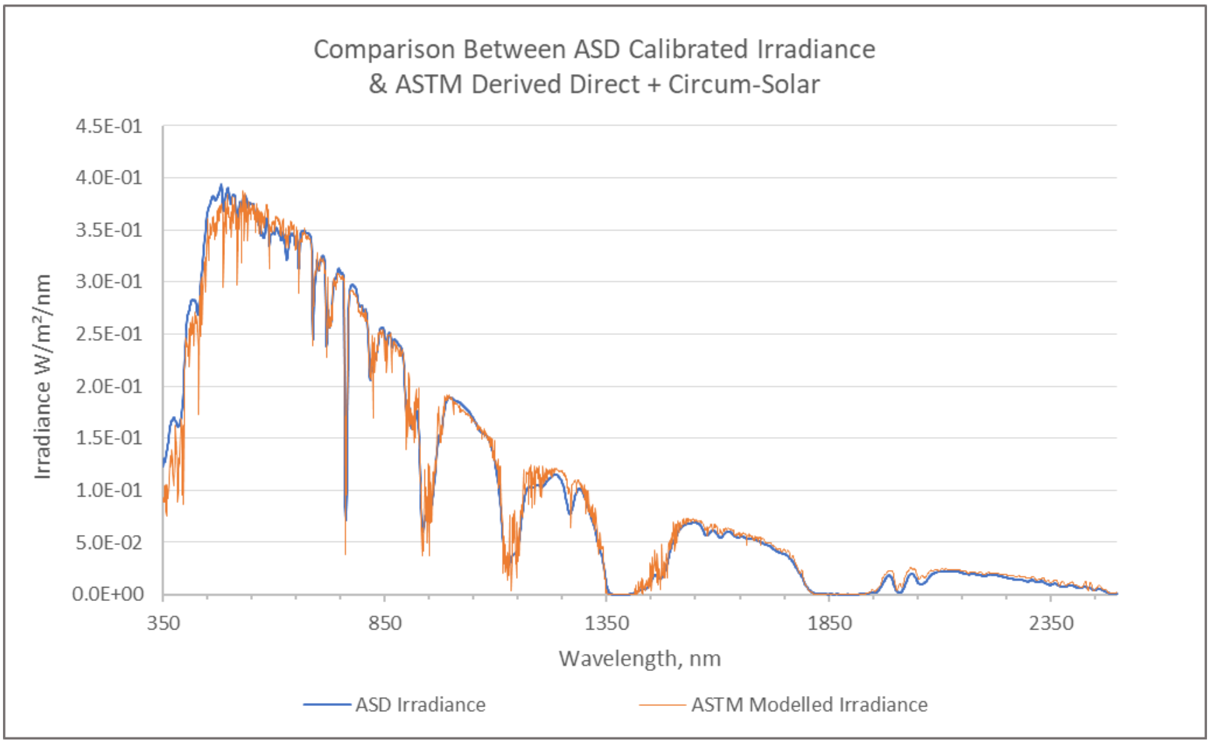

Figure 13: Scaled ASD Irradiance values plotted for comparison against ASTM derived model

It can be seen in Figure 13 that the ASD is potentially overreading slightly in the blue and UV region, but this could be due to the low angle of the winter Sun while these field measurements were acquired. It should also be noted the spectral resolution of the system at 400 nm is ~10 nm whereas at 700 nm it us < 3 nm.

3.5 Spectral Calibration

3.5.1 Verification of the Spectral Calibration

The ASD spectroradiometer uses a third-order polynomial to calibrate the spectral sampling points within its three spectrometers, as mentioned in Section 3.1. The coefficient values for each of the five, third order polynomials are saved in the asdcfg.ini file and uploaded into the instrument's non-volatile memory. During an acquisition the instrument allocates the wavelength value to each sample point. This data is then spectrally interpolated to a 1 nm interval.

The first step when analysing and characterising the performance of the ASD for the Lunar LIME project is to verify this spectral calibration. Five spectral emission line lamps, (Ar, Hg-Ar, Kr, Ne & Xe) were used. Data interpolation can be disabled for this measurement, but previous measurements have shown good spectral agreement between interpolated & non-interpolated data. Each lamp in turn is placed into an integrating sphere and powered by a DC arc lamp power supply. The output port of the integrating sphere is larger than the field of view of the ASD's fore- optic lens. This ensures that all fibers are equally illuminated without biasing the spectral data (example of response for each lamp in Figure 14). The measurements can also be repeated without the large 1 ° FOV lens and with the emission lamps placed close to the tip of the fore-optic scrambler. This increases the signal intensity and improves the SNR for many of the SWIR 1 & SWIR 2 emission lines (Figure 15).

All ASD data converted to ASCII and saved into the Excel spreadsheet for analysis and Gaussian fitting.

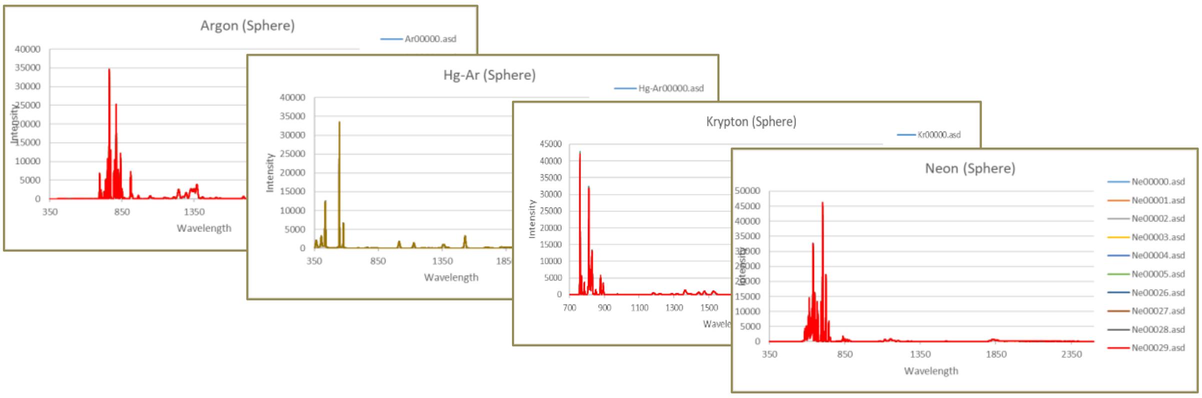

Figure 14: Spectral response plotted for each lamp Ar, Hg-Ar, Kr, Ne

Note each analysis page includes a macro button to run Solver's Gaussian fit.

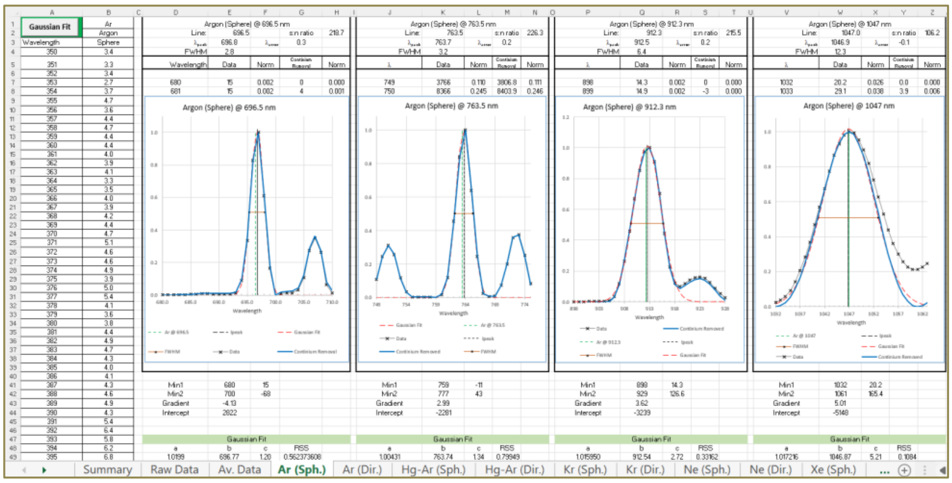

Figure 15: Chosen peaks for each spectral lamp are isolated for comparison

Summary of calibration uncertainties for the strong emission lines from the lamps is shown with the weak and multiple lines[3] excluded for both direct lamp viewing (Figure 16) and sphere source viewing (Figure 17).

[3] NIST Atomic Spectral Database https://www.nist.gov/pml/atomic-spectra-database

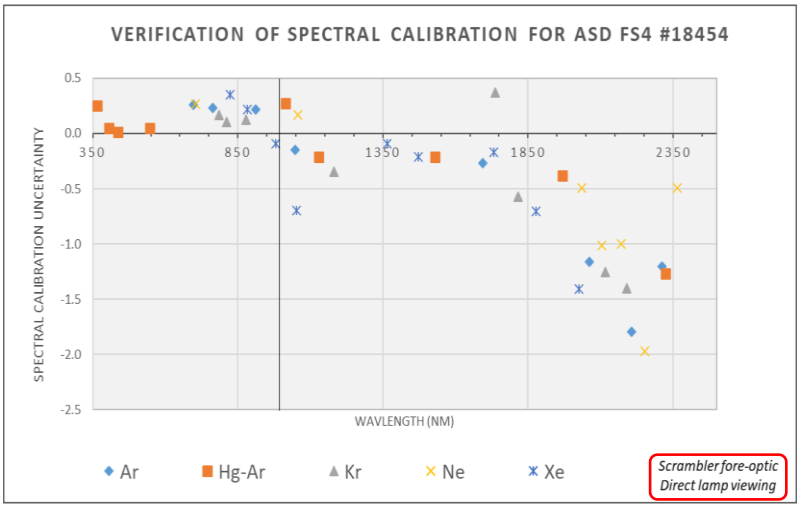

Figure 16: Verification of Spectral Calibration with scrambler fore-optic and direct lamp

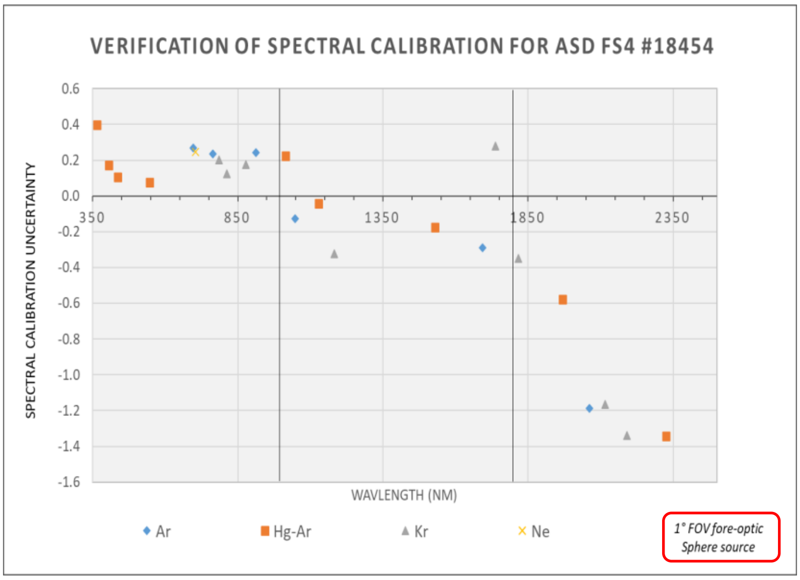

Figure 17: Verification of Spectral Calibration with 1 degree FOV and sphere source

At first glance it may seem that there is a significant error in the spectral calibration of the ASD above 1900 nm. However, as will be shown in the next section this uncertainty is significantly smaller than the spectral resolution of the system in the SWIR regions, close to the sampling interval (1.1 to 2.2 nm) and fraught with difficulties including finding suitable strong, isolated, emission lines in this region. A spectral recalibration of the ASD system is not advised as will unlikely reduce spectral calibration uncertainty and may introduce systematic errors linked to the Gaussian method and assumptions.

3.5.2 Spectral Resolution

If we assume the spectral response function for the ASD best approximates a Gaussian response, then it is possible to extrapolate the spectral resolution from the spectral line lamp data. As with the spectral calibration it is necessary to carefully select the spectral emission lines and to ensure there are no secondary lines which would broaden the apparent spectral resolution. It should be noted that the spectral resolution would not normally fluctuate over a short spectral distance, and this can be used as secondary indicator of erroneous multi-emission lines.

Figure 18 below is taken from the Hg-Ar emission line lamp data in the Excel spreadsheet. The Gaussian fit shown in red is used to model the spectral response of the ASD at three of the mercury emission lines. The half-height of this fit (orange line) equates to the spectral resolution of the system (FWHM) at that wavelength.

From the expression of a Gaussian model:

$$f_{(x)} = a * e^{-\frac{(x-b)^2}{2c^2}} \qquad 4$$

Where a is the height of the curve peak, e is Euler's number, b is the position of the centre of the peak and c is the standard deviation.

The full width at half maximum:

$$FWHM = 2.35482 * c \qquad 5$$

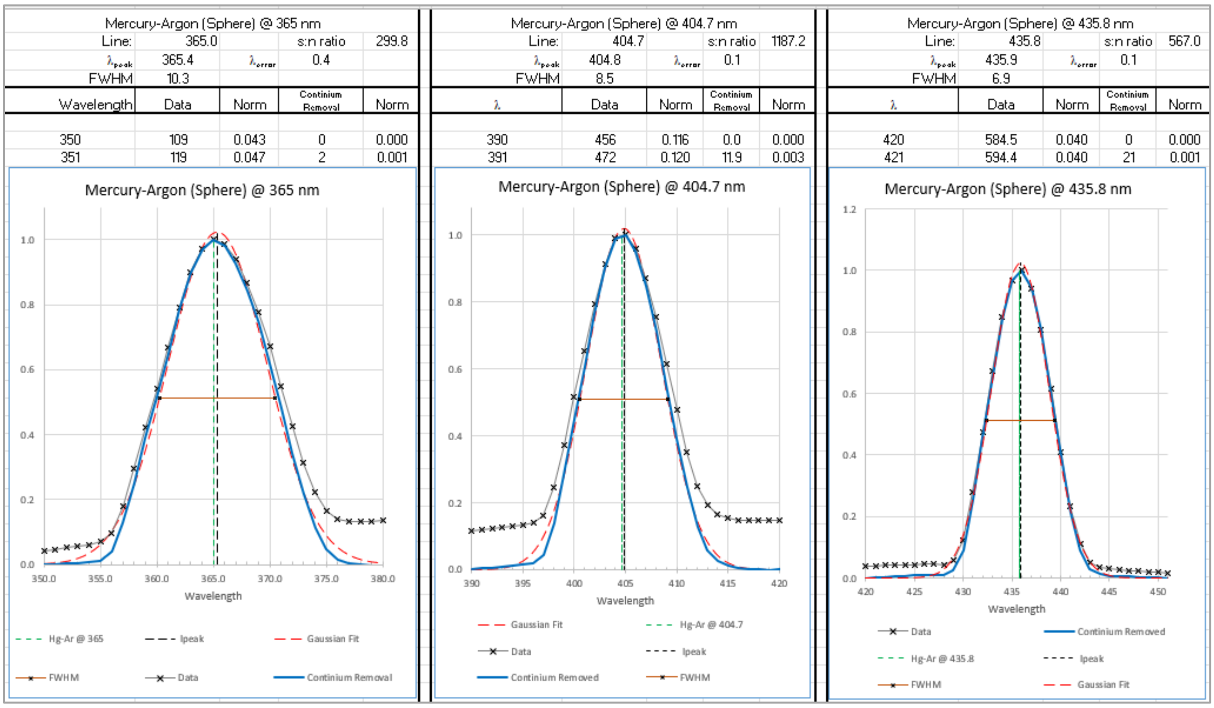

Figure 18: Hg-Ar spectral response Gaussian fitting at 3 separate emission lines, FWHM shown by red horizontal line within each peak

This exercise is repeated at other distinct emission lines to map the spectral resolution across the spectral range of each of the ASD's three spectrometers. It should be noted that these values are based on a Gaussian fit and may differ slightly from other fitting models, designed theoretical values and the manufacturer's specification.

Plotting the FWHM values for the emission lines for the various lamps shows a changing spectral resolution for the VNIR spectrometers with a minimum value of < 3 nm around 700 nm to more than 10 nm in the UV region (Figure 19, Figure 20). This might be explained as a curved image plane across the detector array, with the image only being in focus at 700 nm. The spectral resolution for the SWIR 1 and 2 spectrometers is more constant, though the broad spectral resolution makes selection of isolated emission lines more difficult.

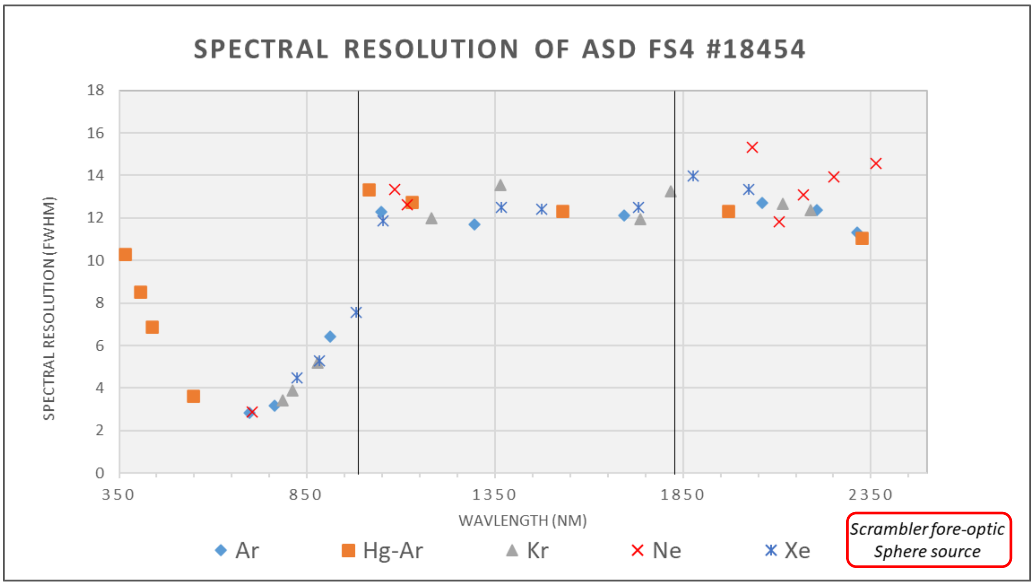

Figure 19: Spectral Resolution with scrambler fore-optic and sphere source

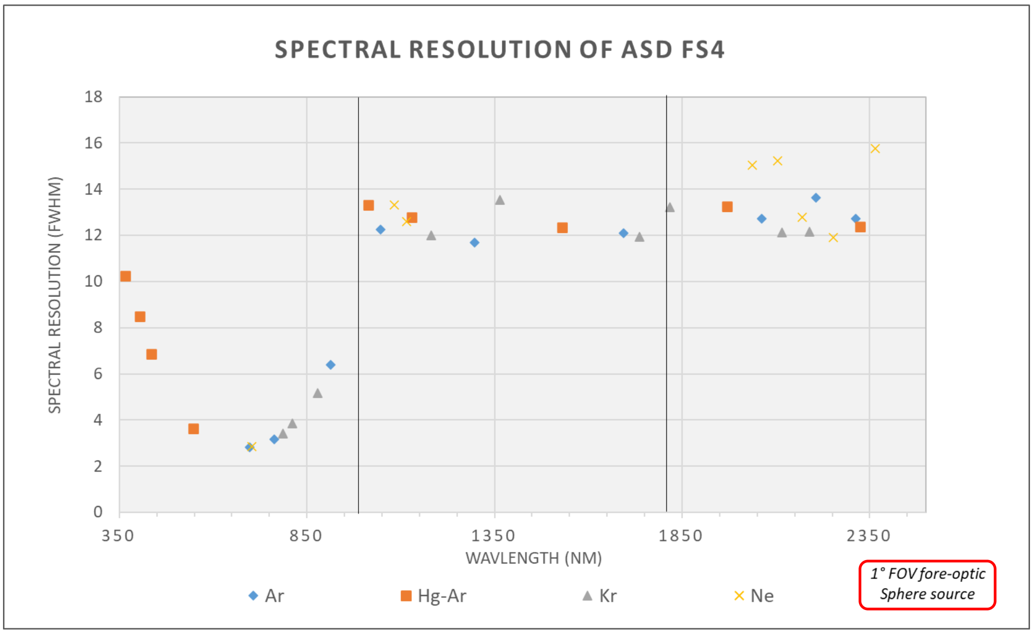

Figure 20: Spectral Resolution with 1 degree fore-optic and sphere source

Table 2 below lists the spectral calibration uncertainty, spectral resolution values and the sampling intervals for the three spectrometers.

Table 2: Spectral Values for each of the 3 internal sensors

	VNIR Spectrometer	SWIR-1 Spectrometer	SWIR-2 Spectrometer
Spectral Uncertainty	0.2 – 0.4 nm	0.2 – 0.4 nm	0.5 – 2.0 nm
Spectral Resolution	3 – 10 nm	12 – 14 nm	11 – 15 nm
Sampling Interval	1.31 – 1.38 nm	1.1 – 2.2 nm	1.1 – 2.2 nm

Reviewing the analysis from lamp spectral data and the system's specification makes it difficult to improve on the factory calibration of this ASD spectroradiometer.

3.6 Directional Response Function for ASD with 1° Field of View and Scrambler

The lunar spectral irradiance measurement requires the field of view of the ASD fore-optics to be larger than the new moon, typically 0.5 °, full angle (0.56 ° at its closest distance to the Earth).

The nominal 1 ° field of view fore-optics has been selected as the most suitable option available for this project. The directional response functions of ASD fore-optic lenses have been shown to be non-uniform with the separation of spatial and spectral features. However, the addition of an optical scrambler between the tip of the optical fibres and lens homogenises the directional response functions (DRF).

The position of the moon within the field of view is dependent on the accuracy of the tracker. During the phases of the moon, its size will grow and diminish. It is therefore necessary to measure and characterise the DRF of the 1 ° fore-optic with its scrambler.

The ASD fore-optics (1 ° lens + scrambler) was mounted to view a small 20 W tungsten halogen lamp at a distance of 4.7 m from the front of the lens. The fore-optics were linear traversed horizontally and vertically to create a raster scan across the FOV. A Raw DN spectral scan was collect at each of the ~300 measurements. For each wavelength the data was normalised to maximum signal and plotted within Excel in a 3D plot. The DRF at four wavelengths are shown here in Figure 21:

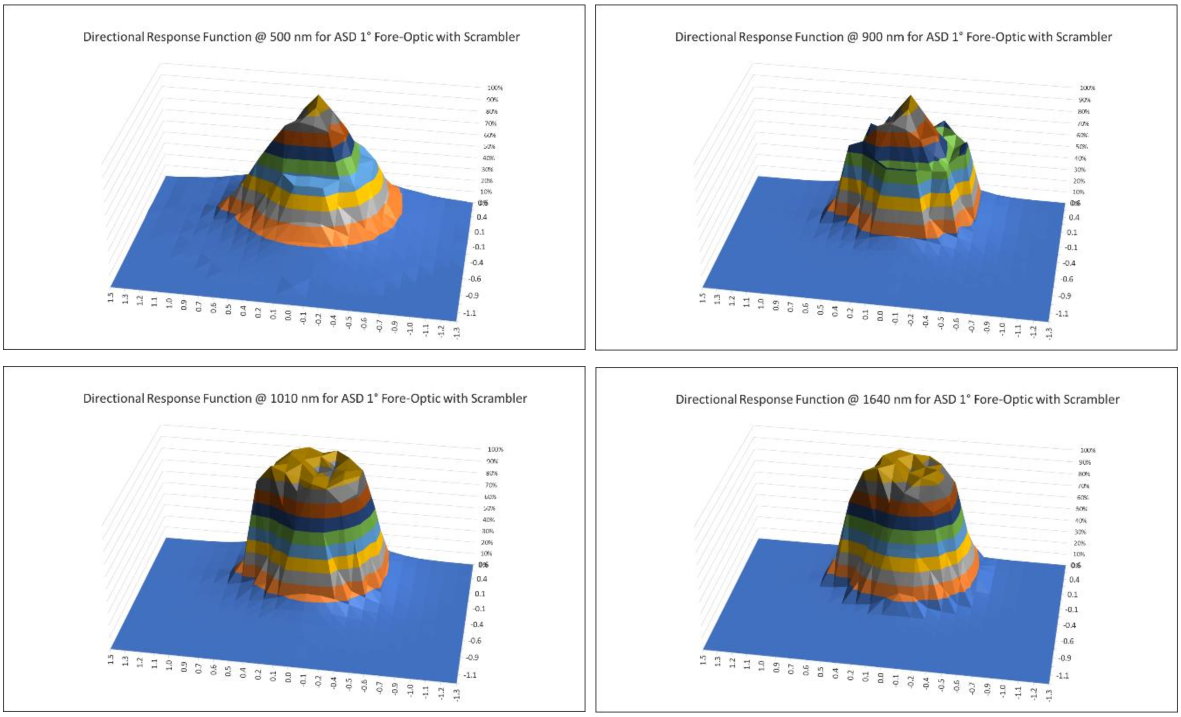

Figure 21: DRF for ASD at wavelength UL - 500nm, UR 900nm, LL 1010nm, LR 1640nm

The DRF of the V-NIR spectrometer appears to have a more variable response across the field of view (Upper Left and Upper Right Figure 21) and this may result in discontinuities between the V-NIR and SWIR-1 spectral regions, depending on the size and position of the moon within the FOV.

This then links to preliminary work done in the Appendix A where a radiance sphere source with variable output port sizes is used to simulate the moon during different phases and aims to quantify the effect of these differences between the DRF data for the three spectrometers within the ASD.

3.7 Thermal Stability

The VNIR detector within the ASD has significant thermal dependencies between 900 nm and 1000 nm ([4]). A temperature stabilised environmental enclosure has been built to house and protect the ASD. The enclosure also includes a temperature data logger set to a 10-minute interval for up to 50 days of data collection. Without thermoelectric (TE) cooling the temperature inside the enclosure rose by +10 C over a 3-hour period. A 40 W air to air thermo-electric cooler and controller has been built on to the enclosure (Figure 22). The TE cooler can stabilise the internal air temperature of the enclosure to within <0.5 ^{o}C. The set point should be optimised to match external ambient temperature more closely.

Figure 22: Example of the thermo-electric cooler (left) and controller (right)

The TE controller is programmable through a USB interface to an application on the ASD computer. The temperature and control settings can be adjusted to the field environmental conditions to give the greatest thermal stability during night-time data collection.

Further details on the enclosure and thermal regulation can be found in Appendix A (Section 5.3).

4 Observational strategy

The hyperspectral measurements should cover "sufficient number of lunar phase angles to capture the possible spectral variability of the lunar disk reflectance with phase angles and libration". Strictly speaking, this requirement would impose for several years of measurements, in a similar way as it is ongoing with the Cimel radiometer. However, in the course of this project (18 months) we need to select, prepare and characterize the instrument, perform the measurements and then analyse the data and incorporate them to the model. Therefore, there is no time to cover the range of libration angles and we can only aim at covering a wide range of phase angles. The analysis of the measurements and their comparison with other available spectral data (rock samples, airLUSI, etc.) will then indicate if the changes in spectral response are small or, on the contrary, if more measurements are needed to ensure the target uncertainty in all possible phase or libration angles.

[4] A. Hueni and A. Bialek, "Cause , Effect , and Correction of Field Spectroradiometer Interchannel Radiometric Steps," *IEEE J. Sel. Top. Appl. Earth Obs. Remote Sens.*, vol. 10, no. 4, pp. 1542–1551, 2017, doi: 10.1109/JSTARS.2016.2625043

In this way, we propose an intensive campaign of 3 lunar cycles, to be held in the time of the year with best atmospheric conditions at Izaña Observatory, regarding low aerosol content and clear skies, i.e. April to June. Prior to this observation period, the selected instrument will be tested by UVa in the field (Valladolid roof platform), to verify that the measurement system as a whole –spectrometer, enclosure, tracker, acquisition software– works properly.

UVa and AEMET staff will operate the instrument at Izaña during the observation period and will take advantage of the radiometric laboratory there to check for radiometric stability before and after each lunar cycle, and whenever the instrument needs to be taken down due to bad weather.

A wide set of ancillary atmospheric observations at Izaña observatory are available to the project, and will be used to control the data quality in real time. This is critical during the campaigns in which each piece of data is important. The data will be revised on a daily basis to early detect any instrument malfunction.

5 Appendix A

5.1 Validation of 1º FOV at Varying Distances

Additional measurements were taken of the ASD fore optics (1 ° FOV plus scrambler) to re-affirm the specified viewing angle can be extended to greater distances.

The fore optic was back-lit with a fiber source and projected onto graph paper at varying distances (Figure 23). The diameter of the images are plotted below (Figure 24) together with a linear fit for distances greater than 3 meters from the fore-optic lens.

It can be confirmed that beyond 3 m distance the 1 º FOV behaves as expected and exhibits a 0.968 º FOV.

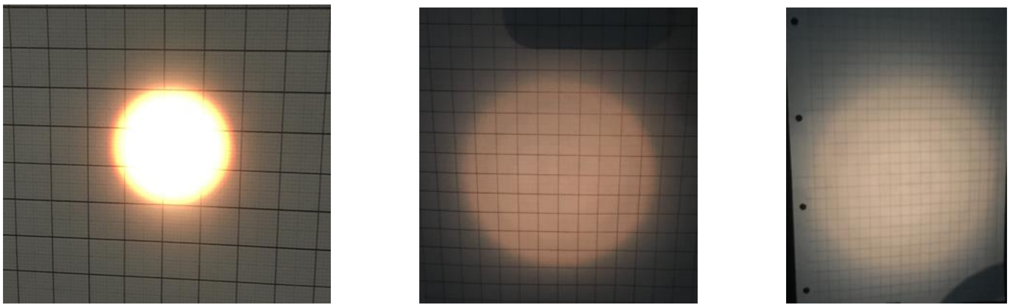

Figure 23: Back-lit ASD fore optic with scramble at increasing distances

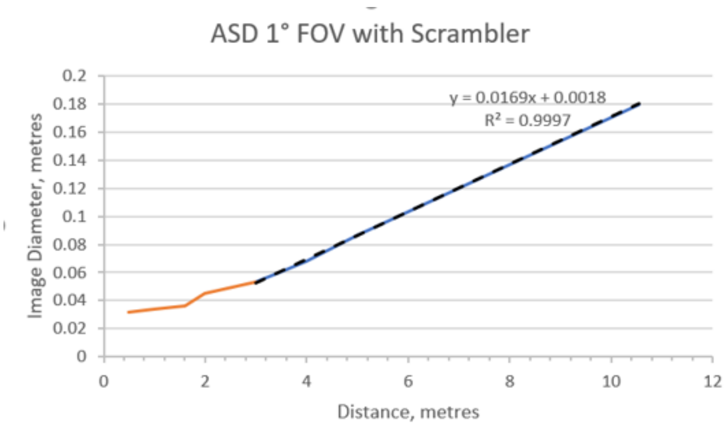

Figure 24: Validation of 1 degree FOV size with varying distance

5.2 Preliminary Data Regarding Lunar Simulation and Directional Response Sensitivity

As we have seen above there is some non-uniformity in the directional response across the field of view (Section 3.6), particularly in the VNIR where it was necessary to examine the variation in the spectral response with different simulated lunar phases. Using a radiance sphere source with a 38 mm ϕ output port, and a variable iris aperture, the relative changes to system response at different iris aperture diameters (2 – 45 mm) were observed.

The 18 mm iris aperture simulates the full moon with everything below this representing reduced lunar disc size. The data below displays each aperture size from 2 mm – 18 mm ratioed against the 18 mm aperture (Figure 25). With a relative radiometric calibration based on the 18 mm 'full moon' the results are relatively linear, only displaying a slight step between each sensor.

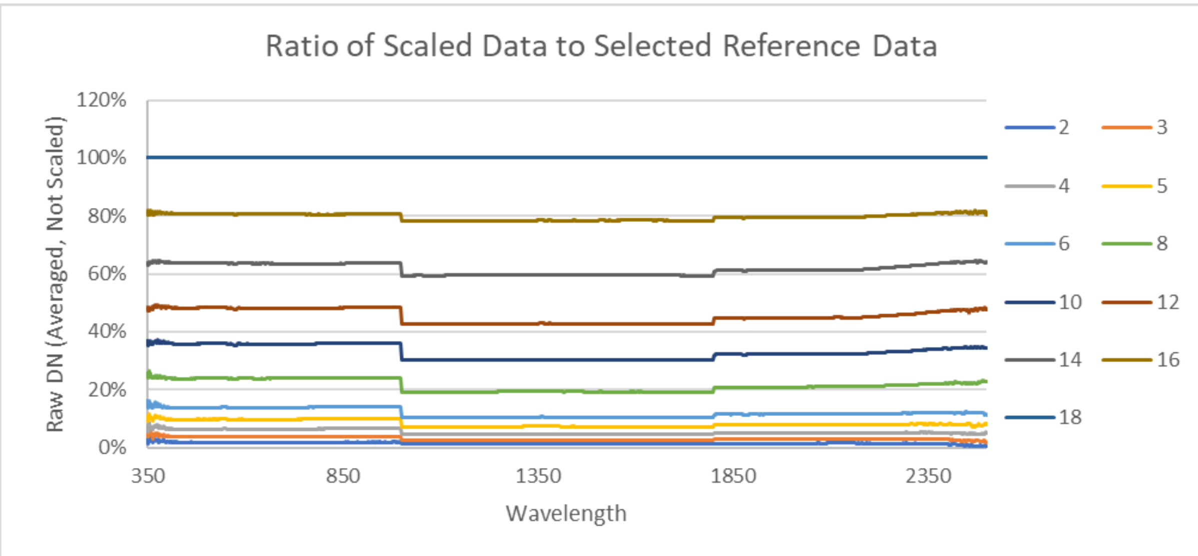

Figure 25: Scaled data at smaller apertures 2mm - 18mm, ratioed against 18mm (full moon) aperture size

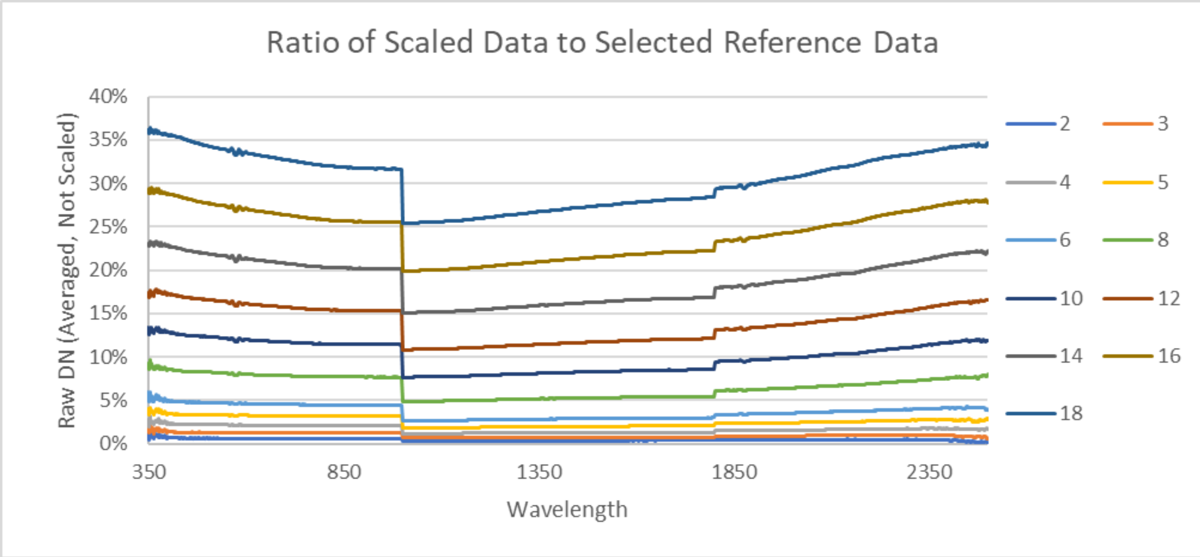

Figure 26: Scaled data at smaller apertures 2mm - 18mm, ratioed against 40mm (overfilling FOV) aperture size

When these same simulations are compared against a larger than 'full moon' aperture (e.g. 40 mm) the step becomes significantly larger, particularly in the VNIR region (Figure 26). The calibration linear offsets appear to be less significant if the calibration is performed on the 'full moon' as opposed to the overfilled field of view. This approach could be further refined by modelling the changes in relative response.

When considering the relative radiometric calibration, as discussed in Section 3.3, it may be necessary to select radiometric calibration factors which minimize any step in the spectral irradiance data at 1000 nm and 1800 mm. This will be explored in further detail when data is acquired from the field testing. It is important to note that for all radiometric calibration the CIMEL data will provide a significant anchor against which to compare these new hyperspectral calibration data.

5.3 Enclosure Design and Software Development

As discussed in Section 3.7, the temperature stability of the ASD is essential if we want reliable data. We were unable to purchase a commercial enclosure with heater/cooler it was necessary to build a bespoke housing to regulate the temperature of the ASD and protect the 1.5 m optical fiber and fore optic. A sealed flexible conduit links the enclosure to the new fore-optic housing (design pictured in Figure 27). It is also necessary that the fiber and its protective conduit can accommodate the required movement of the lunar tracker during use.

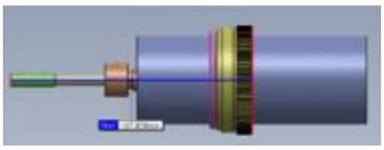

Figure 27: FOV and scrambler fore-optic housing design

The original plan was to house the main components, including the TE cooler/heater, programmable controller, and data logger inside a 210 mm x 500 mm x 500 mm enclosure allowing comfortable air flow inside the enclosure (Figure 28). This enclosure would then be mounted on a frame or table near the lunar tracker and the cable alone would move with the nightly measurement acquisition.

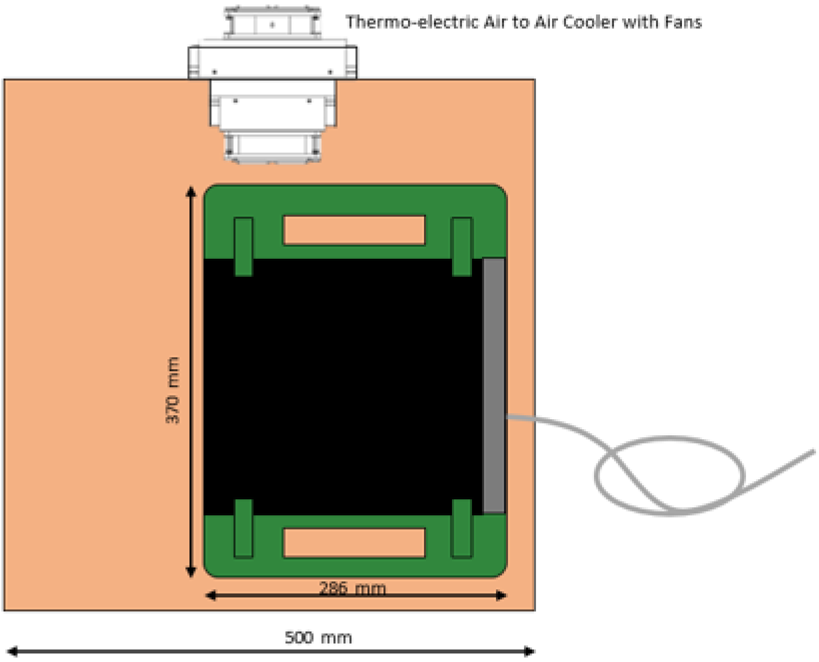

Figure 28: Diagram of original enclosure plan and ASD size within this

However, after discussions with project partners at the University of Valladolid it was suggested that this represented a significant risk to the tangling of the ASD fiber-optic, as has been seen on similar solar tracker systems in the past. Instead, it was decided that a smaller light enclosure would be mounted on the lunar tracker itself with the fiber optic only required to accommodate the zenith rotation of the tracker motion. This also minimizes tangling potential.

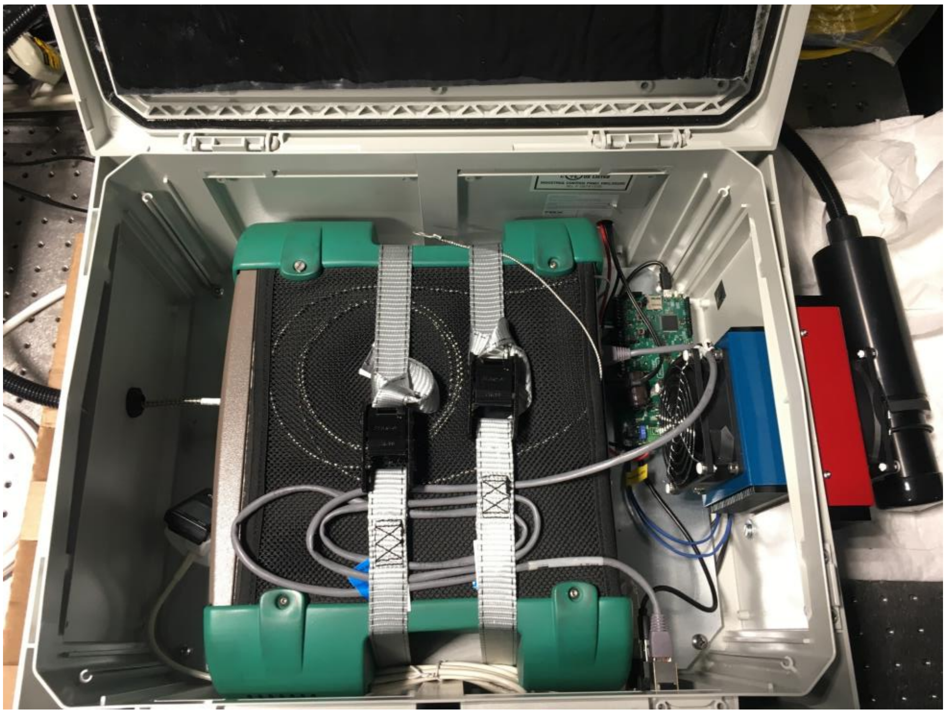

Figure 29: Final ASD enclosure with TE cooling components fitted

As a result of weight restrictions, the ASD and components were rebuilt inside a smaller, lighter plastic enclosure weighing <20 kg (Figure 29). There will also be a separate power supply box with the ASD mains adapter and power supply for the TE 12 V, 100 W power supply (Figure 30).

Figure 30: Smaller, additional enclosure for the power supplies

The ASD will be switched off during the daytime to reduce internal heating while the TE cooler will remain on over the 24 hr period. The temperature for this should be set to maintain overnight temperature with some allowance to exceed the set point during the day. If day temperatures are particularly high, then the enclosure may require some additional shading or cover to reduce the direct heat during the day.

In order to run the ASD a LabView application was developed at NPL to ensure data acquisition and to monitor gain settings throughout the night. Communication from the ASD will be via an ethernet connection as this has proved to be more reliable than the Wi-Fi connection. The application is based on the ASD SDK for LabView and is installed on the ASD laptop, although RS3 will still be available on the laptop as required.

During initial overnight tests >1000 spectra were collected without any issues. AQuick Start Guide has been provided to project partners in the field for use in setup and data collection. An example screenshot of the dark signal can be seen in Figure 31 below.

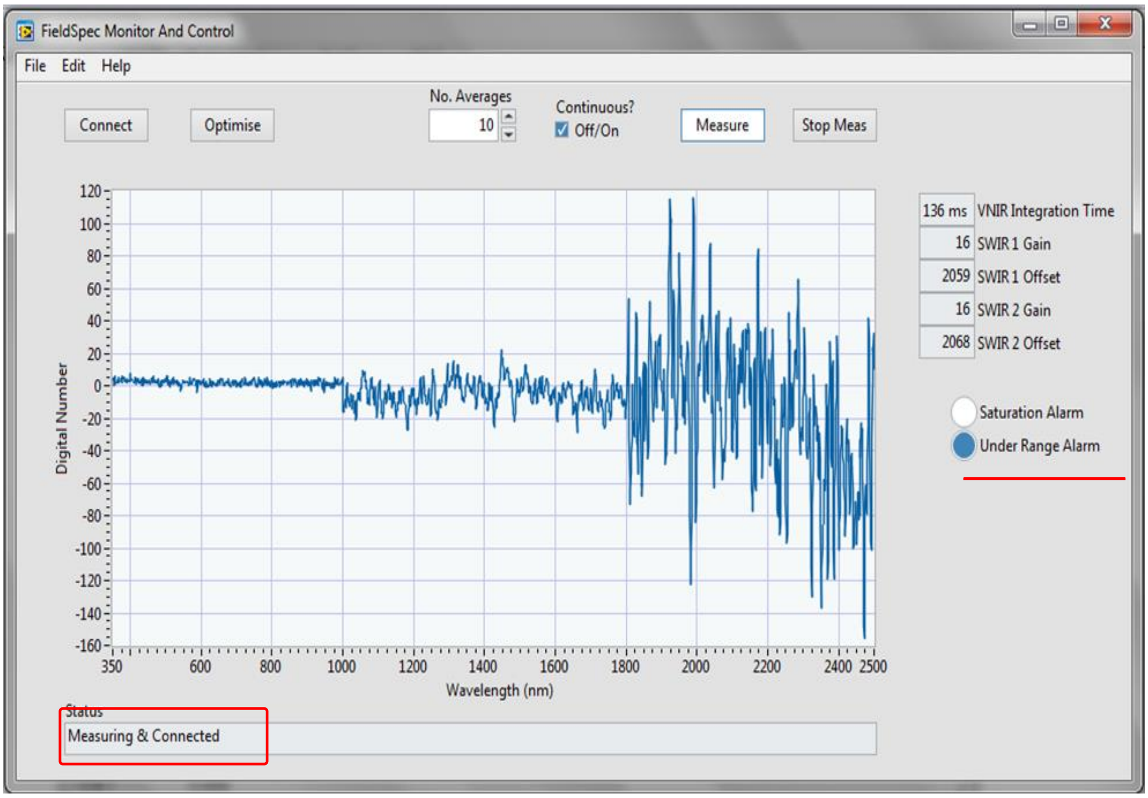

Figure 31: Example interface for LabView software showing active measuring on screen and alarm settings